

THE PITZ CDS BOOSTER CAVITY RF TUNING AND START OF CONDITIONING

V. Paramonov*, A. Naboka, INR of the RAS, Moscow, Russia

A. Donat, L. Jachmann, W. Koehler, M. Krasilnikov, J. Meissner, D. Melkumyan, M. Otevel,

B. Petrosyan, J. Schultze, F. Stephan, G. Trowitzsch, R. Wenndorf, DESY, Zeuthen, Germany

K. Floettmann, DESY, Hamburg, Germany

D. Richter, HZB für Materialien und Energie GmbH, Berlin, Germany

Abstract

The DESY PITZ booster cavity, based on the Cut Disk Structure (CDS), is completed in construction. The L-band normal conducting cavity is intended to operate with accelerating gradient up to $14 \frac{MV}{m}$ and RF pulse length up to $900 \mu s$ to increase the electron bunch energy in the PITZ facility by $\sim 20 MeV$. The cavity was vacuum conditioned to reduce the out-gassing rate for operation in the facility with photo cathodes. The cavity is mounted in the PITZ tunnel and RF conditioning has started. The results of RF tuning before and after cavity brazing together with first results of conditioning are presented.

INTRODUCTION

The normal conducting booster cavity is intended to increase the electron bunch energy in the Photo Injector Test (DESY, Zeuthen) experiments [1]. A normal conducting cavity is selected due to infrastructure particularities in DESY Zeuthen. The multi-cell cavity is based on the CDS compensated accelerating structure with the improved coupling coefficient value. The main design parameters of the cavity are listed in the Table 1.

The cavity scheme, together with diagnostic, pumping and

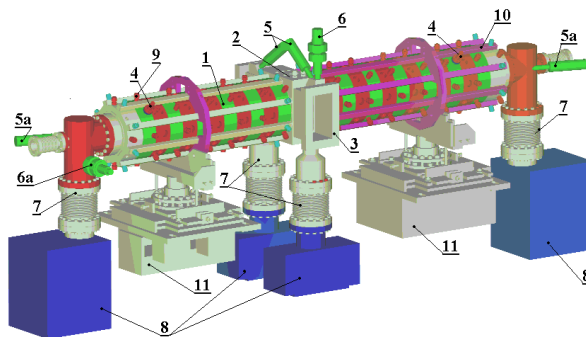


Figure 1: Scheme of the booster cavity. 1 - regular cells, 2 - RF coupler cell, 3 - RF input flanges, 4 - RF probes, 5 - photo multipliers, 5a - reserve photo multipliers, 6 - vacuum gauge, 6a - reserve vacuum gauge, 7 - pumping tubes with bellows, 8 - ion pumps, 9 - internal cooling circuit outlets, 10 - outer cooling circuit, 11 - support and adjustment.

cavity design is described in [2].

CONSTRUCTION AND RF TUNING

The cavity has been constructed and tuned in DESY Hamburg. Initially a cells test program has been performed. Eight half cells were manufactured and RF parameters were measured in a special short test assembly to check precision of manufacturing, sensitivity of frequencies both for accelerating f_a and coupling f_c modes to dimension change, f_a and f_c deviations during the high temperature brazing in vacuum.

The RF tuning before brazing was done for total cavity, including RF coupler cell and two end cells, without individual cells tuning. But cells frequencies f_a and f_c were measured for research purpose, showing relative standard deviation $\sigma_a = 0.003\%$ for the accelerating mode and $\sigma_c = 0.019\%$ for the coupling one. The obtained cavity modes spectrum is shown in Fig. 2 with $f_a = 1300.10 MHz$, $f_c = 1298.35 MHz$, $Q_0 = 18700$ at temperature $20 C^\circ$. There were no tuning of the accelerating field distribution, shown in Fig. 4a and the relative standard deviation $\sigma_E = 1.5\%$ was naturally obtained. The main contribution to the σ_E value in comparison to the practically flat field in regular cavity parts, as one can see from Fig. 4a, is provided from RF coupler cell in the cavity cen-

Table 1: Cavity Design Parameters

Parameter	Unit	Value
Operating frequency	MHz	1300
Particle velocity	relative	1.0
Nominal gradient $E_0 T$	$\frac{MV}{m}$	12.5
Maximal gradient $E_0 T$	$\frac{MV}{m}$	14.0
Nominal energy gain	MeV	20.18
Maximal surface field	$\frac{MV}{m}$	40.0
Maximal RF pulse power	MW	8.6
Maximal RF pulse length	μs	900
Nominal repetition rate	Hz	5
Aperture diameter	mm	30.0
Number of periods		14
Required Q-factor	at $20 C^\circ$	20100
Operating temperature	C°	≈ 44
Residual gas pressure	$Torr$	$\leq 10^{-7}$

cooling equipment, is shown in Fig. 1. In more details the

*paramono@inr.ru

ter and two end cells, which differ in the shape from the regular cells. The obtained σ_E is a natural lower limit for the present cavity design. In more details the results of cells test program and cavity tuning is presented in [3].

Several steps, with silver based alloys, differing in melting

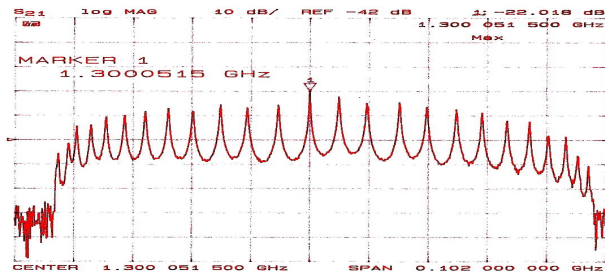


Figure 2: The cavity modes spectrum before brazing.

temperature, have been performed in the brazing of cavity parts. The last step was the brazing of large cavity parts together. The RF tuning of the brazed cavity, Fig. 3, is in frequency tuning and RF probes matching.

The frequency tuning has been performed by outer wall

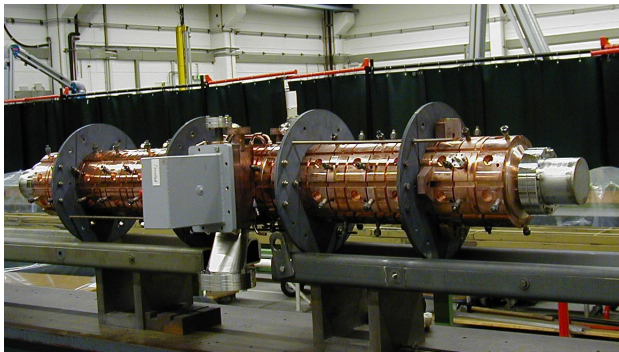


Figure 3: The cavity after final brazing.

deformations in special blind holes, foreseen in each cavity accelerating cell, resulting in the cell frequency increasing. At the first step the frequencies of RF coupler cell and end cells were equalized with frequency of regular accelerating cells. The difference was detected before brazing and tuning of these cells was postponed. At the second step the frequencies of all cells were enlarged at the same value to have for cavity the operating mode frequency $f_a = 1300.145 MHz$ at the temperature $20C^\circ$. Not all blind holes in each cell were deformed, and, if required, the cavity operating frequency can be increased at $\approx 150 kHz$ for operation at higher temperature. The measured distribution of electric field at the cavity axis before brazing, after brazing and after RF tuning is shown in Fig. 4.

Due to several additional steps in cavity brazing the frequency shift for coupling modes is larger than expected. The cavity has the stop band width $\delta f = f_c - f_a = 900 kHz$ and $\frac{\delta f}{f_a} \sim 7 \cdot 10^{-4}$. For the short cavity with $N = 14$ periods for acceleration of relativistic electrons there is to rigid tolerance for δf value and obtained σ_E

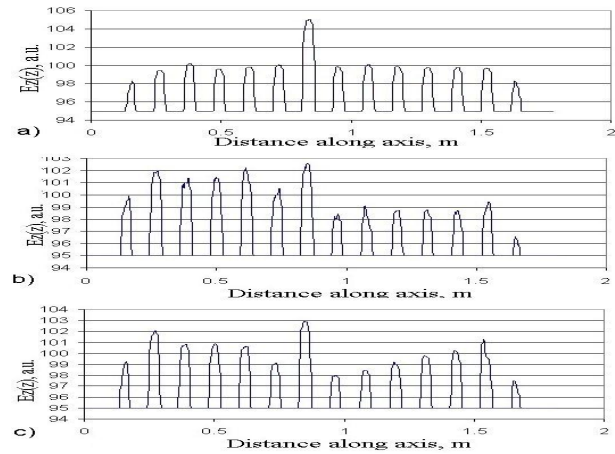


Figure 4: The field distribution along the cavity axis in the enlarged scale before brazing (a), $\sigma = 1.5\%$, after brazing (b), $\sigma = 1.7\%$, and after RF tuning (c), $\sigma = 1.5\%$.

value, see Fig. 4c, is near accessible limit. The cavity is intended to operate with high average heat loading, up to $2.8 \frac{kW}{cell}$ and the enlarged positive stop band width only leads to more thermal stability in operation [4].

The antenna type RF probes were adjusted to have pass-through attenuation of $\sim 71 dB$, resulting in $\sim 0.6 W$ signal power for nominal operation.

The measured quality factor $Q_0 = 21680$ also exceeds expected design value $Q_0^d = 20100$, see Table 1. It is of 92% with respect calculated Q value for regular cells. The cavity is over matched slightly and at the temperature of $20C^\circ$ the measured WSWR value is of 1.33. For operating temperature of $(44 \div 48)C^\circ$ the own quality factor value decreases at $\approx (8 \div 9)\%$, resulting in WSWR reduction to 1.22 and reflection coefficient value is $\rho \approx 0.1$, corresponding to 1% of reflection in RF power.

CONDITIONING

20100531 071529 uhv100 abschluss

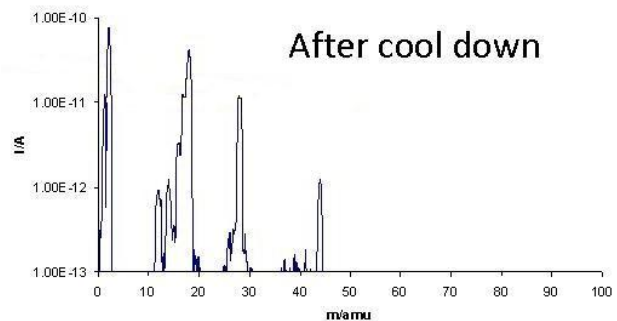


Figure 5: The partial gas pressure after cavity baking.

After delivery to DESY Zeuthen the cavity baking with temperature up to $120C^\circ$ was done during sufficient time to reduce the hydrocarbons partial pressure for the limit,

required for operation in vacuum circuit with photo cathode. The final spectrum of residual gas partial pressure is shown in Fig. 5.

The cavity is installed in the PITZ beam line and all connections are performed, Fig. 6.

The initial stage of RF conditioning has been per-

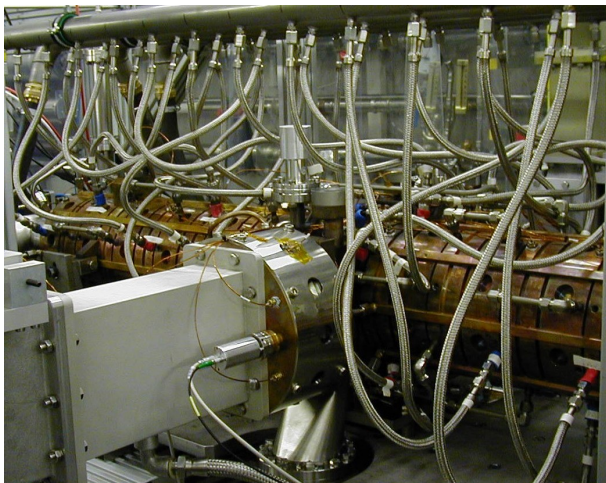


Figure 6: The CDS booster cavity in the PITZ beam line.

formed with application of Automatic Conditioning Program (ACP), developed for RF gun cavities conditioning and adapted with special version for CDS booster. The history of initial conditioning with the RF pulse length of $50\mu s$ is shown in Fig. 7. The rate of RF pulse power increasing was limited by pumping capability to keep the residual gas pressure $\leq 10^{-7} Torr$ and minimize interlocking from pumping system.

The level of RF pulse power of $\approx 3.4 MW$ achieved

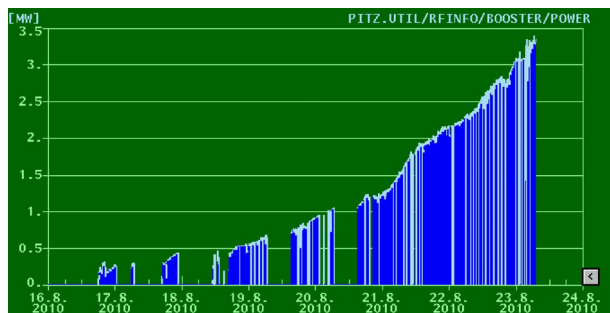


Figure 7: The CDS booster conditioning with automatic conditioning program.

with ACP corresponds to the accelerating gradient $E_0 T \approx 9.3 \frac{MV}{m}$ and the maximal surface field $E_{sm} \approx 28 \frac{MV}{m}$. As one can see from the conditioning history, Fig. 7, no visible problems with multipactor discharge were detected inside achieved level of RF power. Just a limited number of clear RF breakdowns was detected in the achievement of this level. Inside this level of RF power stable operation with longer RF pulse, see Fig. 8, is obtained.

At the moment of this report preparation, up to 5 MW

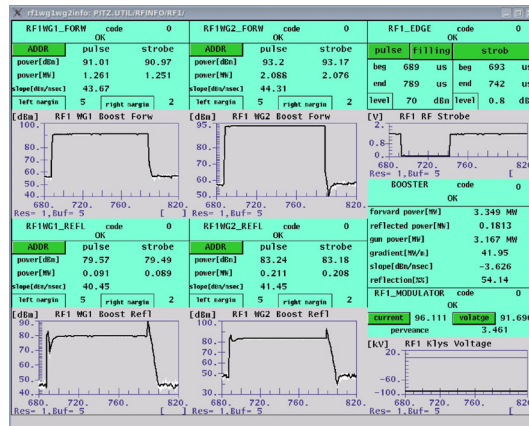


Figure 8: The CDS booster operation with intermediate RF power.

peak RF power in the CDS booster is achieved for short pulse length with limitation by interlocking from reflected RF power at the RF pulse end. More work is required in the fine adjustment of mutual interaction in operation at full RF power both for cavity, including temperature control, powerful RF hardware and control system. This work is in progress.

SUMMARY

The PITZ CDS booster cavity is completed in construction. RF tuning is performed and in measured RF parameters the cavity corresponds to the design requirements. Cavity baking was done to reduce the partial pressure of hydrocarbons to the required level. The cavity is installed in the PITZ beam line and RF conditioning is in progress.

REFERENCES

- [1] A. Oppelt et al., Future plans at the Photo Injector Test Facility at DESY Zeuthen. Proc. 2003 FEL Conference, 18-23 September, Tsukuba, Japan, (2003)
- [2] V.V. Paramonov et al., Design Parameters of the Normal Conducting Booster Cavity for the PITZ-2 Test Stand. Proc. Linac 2004, p. 204, (2004)
- [3] A. Naboka et al, Results of cells test program and cavity tuning at low rf level. Problems of atomic science and technology. ISSN 1562-6016, n. 5, p. 35, (in Russian) (2007)
- [4] L.M. Young, J. M. Potter. CW Side Coupled Linac for the Racetrack Microtron. Proc. PAC 1981, p. 3508, (1983)